

Attaining the PeV frontier of the cosmic ray spectrum in space with HERD

Chiara Perrina^{1,*} on behalf of the HERD Collaboration

¹Institute of Physics, Ecole Polytechnique Fédérale de Lausanne (EPFL), CH-1015 Lausanne, Switzerland

Abstract. The High Energy cosmic-Radiation Detection facility (HERD) is a calorimetric experiment planned to be launched in 2027. It will be operational for at least 10 years on board the China Space Station. With HERD we will measure the energy flux of cosmic protons and heavier nuclei from 30 GeV up to, for the first time in space, a few PeV. We will search for signatures of annihilation and decay products of dark matter in the energy spectrum of cosmic electrons and gamma rays from 10 GeV to 100 TeV. A wide field of view monitoring of the gamma-ray full-sky from 100 MeV will also be performed. The five HERD subdetectors, the calorimeter (CALO), the scintillating fiber tracker (FIT), the plastic scintillator detector (PSD), the silicon charge detector (SCD) and the transition radiation detector (TRD), are currently under development. The design, prospects and expected performance of HERD, as well as its contribution to the multimessenger astronomy will be presented in this contribution.

1 Introduction

- The most accurate values of the cosmological parameters, provided by the Planck mission [1], show that about 84% of the matter present in the universe consists of dark matter. Nevertheless, it has not yet been detected and its nature, origin and properties are still unknown. A method to detect the dark matter is the search for its annihilation and decay products in space, which may produce unique features in the cosmic electron (plus positron) and gamma-ray energy spectra.
- The indirect cosmic-ray measurements performed with ground-based experiments reveal a steepening in the all-particle spectrum between 1 PeV and 10 PeV. The origin of the so-called “knee” of the spectrum is still not clear. Assuming that cosmic rays below 10^{18} eV have Galactic origin, the knee could indicate that most cosmic accelerators in the Galaxy have reached their maximum energy to accelerate protons [2]. Direct measurements in space of the flux and composition of cosmic rays in the PeV region will shed light on the knee origin and the acceleration and propagation mechanisms of cosmic rays.
- Several new populations of extreme astrophysical objects were discovered by wide field of view (FOV) gamma-ray space telescopes in the GeV energy range, and by narrow FOV gamma-ray ground telescopes in the hundreds GeV range. In particular, the wide FOV

*e-mail: Chiara.Perrina@epfl.ch

space telescopes often provide crucial guidance on the observations of ground telescopes. The most powerful ground-based Cherenkov Telescope Array (CTA) [3] currently under development may not have the needed guidance once the Fermi-LAT satellite [4] will stop operations. A new wide FOV space gamma-ray telescope is therefore urgently needed.

Starting from 2027, the planned launch year, and for at least 10 years, HERD will be on board the China Space Station to address the above major problems in fundamental physics and astrophysics. Thanks to its unprecedented acceptance, HERD will open the opportunity to investigate cosmic rays at energies never attained before in space.

2 HERD physics observables and objectives

2.1 Cosmic Electrons and Positrons

HERD will perform high statistics precise measurements of the electron plus positron (CRE) flux up to about 100 TeV. The study of the CRE flux above 1 TeV is very interesting because electrons from 100 GeV lose energy via inverse Compton scattering and synchrotron radiation and therefore have a limited propagation distance. Electrons above few TeV are expected from local sources (< 1 kpc distance) or from dark matter annihilation and/or decay. Fig. 1 (left) shows the expected CRE as measured by HERD with five years of data. HERD will be able to detect spectral cutoff at high energy and local astrophysical sources. High precision measurements of AMS-02 [5] confirmed a rise from 8 GeV to 500 GeV in the positron fraction first revealed by PAMELA [6] that could be consistent with an astrophysical origin or a dark matter origin of positrons. The recent DAMPE result in the CRE spectrum shows a break at 0.9 TeV [7], that could be explained with the existence of an energy limit of the cosmic electron spectrum [8]. In that case, the cutoff of the positron spectrum should be below 0.9 TeV as seems to be favored by the AMS-02 measurements [9]. A way to clarify the origin of the positron excess is to measure the fine structure of the CRE spectrum with a high precision. As shown in Fig. 1 (right) HERD will clearly distinguish between a smooth spectrum, due to a pulsar wind nebula (PWN), or a spectrum with a “kink”, due to dark matter with one year of data.

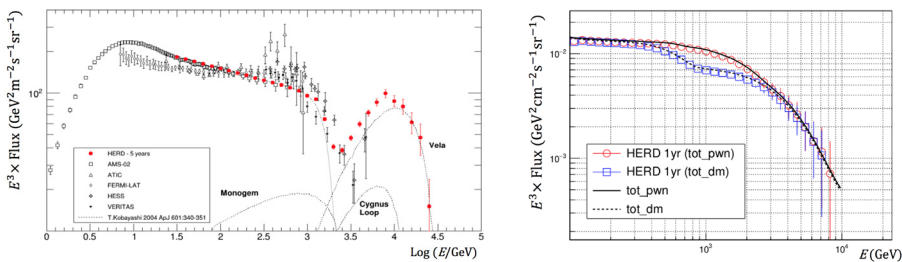


Figure 1: Expected $e^- + e^+$ spectrum as measured by HERD with five years (left) and one year (right) of data.

2.2 Cosmic nuclei

HERD will measure the flux of protons and helium nuclei up to a few PeV and of heavier nuclei (at least up to iron) up to a few hundreds of TeV/nucleon thus providing insights into the production, acceleration and propagation mechanisms of cosmic rays. HERD will

explore directly in space the “knee” of the all-particle flux: the region where ground-based experiments observed a change of the spectral index, that could indicate the confinement limit of high energy particles by the galactic magnetic field, and the contribution of extragalactic sources. Fig. 2 shows the simulated proton (left) and helium (center) energy spectra and boron-to-carbon flux ratio (right) as measured by HERD with five years of data.

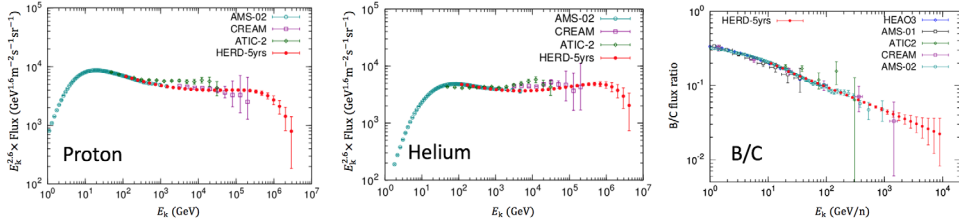


Figure 2: Expected proton (left) and helium (center) energy spectra and boron-to-carbon flux ratio (right) as measured by HERD with five years of data.

2.3 Cosmic gamma rays

Thanks to its large acceptance and sensitivity, HERD will be able to perform a gamma-ray full-sky survey from 100 MeV to study galactic and extragalactic gamma-ray point sources and diffuse emission, as well as the high energy gamma-ray transient phenomena. In the era of multimessenger and multiwavelength astronomy, it is essential to monitor the high energy gamma-ray sky in space, as was demonstrated by the Fermi-LAT detection [10] of the electromagnetic counterpart of the gravitational wave from a binary neutron star merger detected by LIGO. HERD with its unusual large field of view and energy coverage will play a unique role in multiwavelength studies across the electromagnetic spectrum, complementary to other space and ground telescopes measuring radio, optical, X-ray and gamma-ray signals. Its role will also be unique in the search for the electromagnetic counterpart of gravitational waves (detected by LIGO [11], Virgo [12], KAGRA [13]) and neutrino events (detected by IceCube [14], KM3NeT [15]). HERD will produce alerts for active galactic nuclei, novae and binary systems. The sky map expected from HERD after five years of activity is illustrated in Fig. 3. Another particularly interesting detection objective of HERD is the search for dark matter in the gamma-ray spectrum. Two-body dark matter annihilation or dark matter decay could be observed as a sharp peak over the high energy diffuse gamma-ray background. The gamma-ray line feature is considered as the “smoking gun” signal of dark matter. HERD will perform the gamma-ray line search from 10 GeV to 100 TeV with the best sensitivity ever achieved.

3 The HERD detector

The HERD detector (Fig. 4) consists of a 3D calorimeter (CALO), surrounded on the four lateral sides and on the top side by a sector of the scintillating-fiber tracker (FIT), the plastic scintillator detector (PSD), and the silicon charge detector (SCD); a transition radiation detector (TRD) is placed on one lateral side. With this 3D configuration, the total geometric factor of HERD is about 10 times larger than that of current-generation detectors. HERD will have a mass < 4000 kg, with an overall volume of $\sim 3.0 \times 2.3 \times 1.7 \text{ m}^3$. The design of the HERD detector was also studied to reduce the systematic uncertainties (especially on the

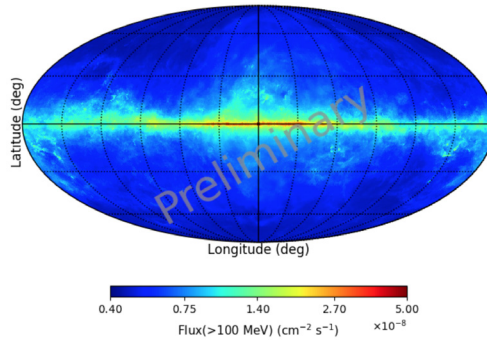


Figure 3: Expected map of the gamma-ray sky [16] in galactic coordinates with five years of HERD data.

absolute energy scale). For this purpose TRD calibrates the response of the calorimeter to high energy hadronic showers and each cube of CALO is read out by two independent systems: a IsCMOS camera and two photodiodes. SCD is the outermost detector to measure the particle charge before any possible nuclei fragmentation. The HERD expected performance in terms of energy range, energy, angular and charge resolution, electron/proton separation and geometric factors are listed in Table 1.

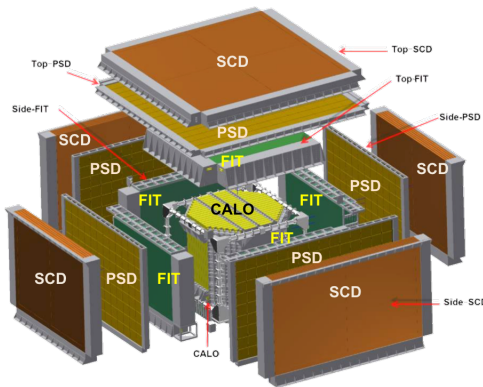


Figure 4: Exploded view of the HERD detector.

3.1 The calorimeter (CALO)

CALO [17] is a 3D homogeneous, isotropic and finely segmented calorimeter which accepts particles coming from every direction but the bottom side that is blocked by the device services and mechanical support. CALO is made of about 7500 LYSO cubes with edge length of 3 cm arranged in a sphere-like shape (Fig. 5) with a total depth of about 55 radiation lengths and 3 nuclear interaction lengths. The scintillation light induced by charged particles in the crystals is read out by two independent systems: the first one consists of wavelength shifting fibers (WLS) coupled to image Intensified scientific CMOS (IsCMOS) cameras, the second one is made of photodiodes [18] connected to custom front-end electronics chips called

Table 1: Expected HERD performance

Energy range (e/ γ)	10 GeV - 100 TeV
Low energy range for γ	100 MeV - 10 GeV
Energy range (nuclei)	30 GeV - few PeV
Angular resolution (e/ γ)	0.1° at 10 GeV
Charge resolution (nuclei)	10% - 15% for $Z = 1 - 26$
Energy resolution (e/ γ)	< 1% at 200 GeV
Energy resolution (p)	20% at 100 GeV - PeV
e/p separation power	> 10 ⁶
Field of view	$\pm 90^\circ$
Geometric factor (e)	> 3 m ² sr at 200 GeV
Geometric factor (p)	> 2 m ² sr at 100 GeV

HIDRA. The double read-out system allows for redundancy, independent trigger, and cross calibration to reduce the systematic uncertainties.

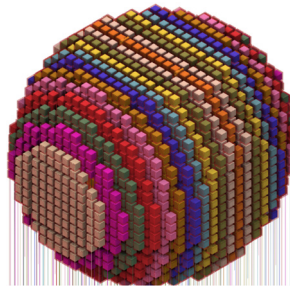


Figure 5: Sketch of the sphere-like crystal array of the HERD calorimeter.

3.2 The scintillating-fiber tracker (FIT)

FIT [19] consists of five tracking sectors, made of 7 tracking planes, for 7 independent measurements of the position of a traversing charged particle (Fig. 6). Each tracking plane consists of two layers of FIT modules measuring the two orthogonal spatial coordinates. A module includes one scintillating-fiber mat and three silicon photomultiplier (SiPM) arrays to read out the scintillation light induced by the charged particles hitting the mat. The mat is made by stacking 6 layers of fibers for a width of 97.8 mm to match three Hamamatsu S13552-10 SiPM arrays. The fibers, manufactured by Kuraray (type SCSF-78MJ), have a round section with an average total diameter of 250 μm with a polystyrene core surrounded by two claddings. FIT aims at reconstructing the trajectories and the charge absolute value of charged cosmic rays, favor the conversion of low energy gamma rays and reconstruct the tracks of the produced electrons and positrons. Simulation studies are being conducted to optimize the tracker performance in terms of geometrical acceptance, angular resolution and converting capability while simultaneously being mechanically stable and complying with the thermal and power requirements set by the space station. In this configuration, FIT has 225792 read-out channels. So far the 128 channels of each SiPM array of FIT prototypes are read out by two VATA64 HDR16.2 ASIC chips made by IDEAS. A dedicated ASIC, called

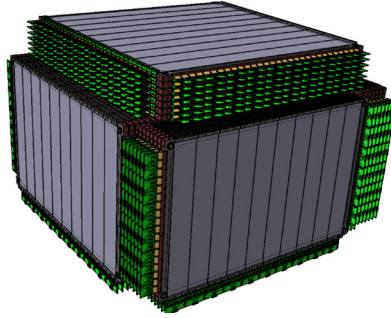


Figure 6: Sketch of the HERD scintillating-fiber tracker (FIT).

BETA [20], with a larger dynamic range and a power consumption less than 1 mW/channel is being developed by the Institute of Cosmos Sciences of the University of Barcelona. BETA will have a dynamic range sufficient for charge measurements up to $Z = 26$.

3.3 The plastic scintillator detector (PSD)

PSD [21] will discriminate incident photons from charged particles, and measure the charge of the latter up to $Z = 26$. The five faces of PSD envelope the five FIT sectors. Its design is being optimizing to achieve a high efficiency in the charged particles detection ($> 99.98\%$), a high dynamic range to identify nuclei at least up to iron, a good segmentation to reduce the back-scattering particles from the calorimeter.

3.4 The silicon charge detector (SCD)

SCD is the HERD subdetector designed to accurately measure the cosmic ray absolute charge magnitude, thus separating chemical species from hydrogen to iron and beyond. SCD is composed of 4 x-y layers of single-sided silicon micro-strip sensors, for 8 independent ionization energy loss measurements per sector. It is the outermost detector to avoid early charge-change interactions in PSD and to reduce the systematic uncertainty on the reconstructed charge due to the nuclei fragmentation. It is highly segmented to minimize the unavoidable backscattered secondary particles coming from the calorimeter. The SCD charge measurement performance has been studied with a Monte Carlo simulation of the full detector. Several proton, helium, carbon, oxygen, silicon, and iron nuclei samples with energies from 10 GeV/nucleon to 1 TeV/nucleon and with isotropic incidence were simulated. It was found (Fig. 7) that the combined charge resolution of 8 layers is below 0.2 charge units for all samples. Design choices for SCD, like the strip pitch and the distance between SCD and PSD, will also be studied in order to minimize the effect of pile-up in charge measurement due to back-splash particles emerging from interactions in the calorimeter. Additionally, SCD is capable of 3D tracking and will be used together with FIT for the particle track reconstruction.

3.5 The transition radiation detector (TRD)

TRD [22] is needed to calibrate the response of the calorimeter to high energy hadronic showers. Space calorimeters can be calibrated on ground only up to 400 GeV using the CERN SPS beam. TRD is used to evaluate the CALO response from 1 TeV to 10 TeV. The TRD is conceived around a modular design, involving a transition radiation radiator and a thick gaseous electron multiplier (THGEM) with an effective area of $20 \times 20 \text{ cm}^2$.

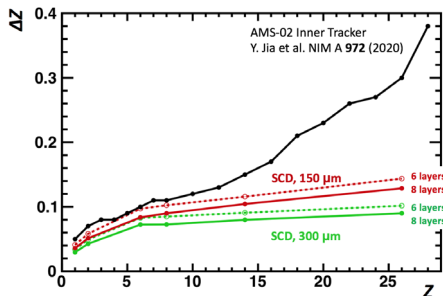


Figure 7: Simulated charge resolution of a SCD sector made of 6 and 8 layers of silicon micro-strip sensors with a thickness of 150 μm and 300 μm as a function of the nuclei charge Z . The charge resolution of the AMS inner tracker is also shown for comparison.

4 Conclusions

HERD will operate on board the China Space Station from 2027 for at least 10 years. The main scientific objectives of HERD include the indirect search for dark matter in the electron plus positron and gamma-ray spectra, the study of the gamma-ray sky, the detection of cosmic electrons and positrons, protons and heavier nuclei to understand the origin, acceleration and propagation of cosmic particles.

5 Acknowledgments

The author gratefully acknowledges the financial support from the Swiss National Science Foundation (SNSF-PZ00P2_193523).

References

- [1] N. Aghanim, Y. Akrami, M. Ashdown, J. Aumont, C. Baccigalupi, M. Ballardini, A.J. Banday, R.B. Barreiro, N. Bartolo, S. Basak et al. (Planck Collaboration), *Astronomy&Astrophysics* **641**, A6 (2020)
- [2] R.L. Workman, V.D. Burkert, V. Crede, E. Klempt, U. Thoma, L. Tiator, K. Agashe, G. Aielli, B.C. Allanach, C. Amsler et al., *Progress of Theoretical and Experimental Physics* **2022** (2022)
- [3] B. Acharya, M. Actis, T. Aghajani, G. Agnetta, J. Aguilar, F. Aharonian, M. Ajello, A. Akhperjanian, M. Alcubierre, J. Aleksić et al. (CTA Collaboration), *Astroparticle Physics* **43**, 3 (2013)
- [4] W.B. Atwood, A.A. Abdo, M. Ackermann, W. Althouse, B. Anderson, M. Axelsson, L. Baldini, J. Ballet, D.L. Band, G. Barbiellini et al. (Fermi-LAT Collaboration), *The Astrophysical Journal* **697**, 1071 (2009)
- [5] L. Accardo, M. Aguilar, D. Aisa, B. Alpat, A. Alvino, G. Ambrosi, K. Andeen, L. Aruda, N. Attig, P. Azzarello et al. (AMS Collaboration), *Physical Review Letters* **113**, 121101 (2014)
- [6] O. Adriani, G.C. Barbarino, G.A. Bazilevskaia, R. Bellotti, M. Boezio, E.A. Bogomolov, L. Bonechi, M. Bonghi, V. Bonvicini, S. Bottai et al. (PAMELA Collaboration), *Nature* **458**, 607 (2009)

- [7] G. Ambrosi, Q. An, R. Asfandiyarov, P. Azzarello, P. Bernardini, B. Bertucci, M.S. Cai, J. Chang, D.Y. Chen, H.F. Chen et al. (DAMPE Collaboration), *Nature* **552**, 63 (2017)
- [8] K. Fang, X.J. Bi, P.F. Yin, *The Astrophysical Journal* **854**, 57 (2018)
- [9] M. Aguilar, L. Ali Cavasonza, G. Ambrosi, L. Arruda, N. Attig, P. Azzarello, A. Bachlechner, F. Barao, A. Barrau, L. Barrin et al. (AMS Collaboration), *Phys. Rev. Lett.* **122**, 041102 (2019)
- [10] M. Ajello, A. Allafort, M. Axelsson, L. Baldini, G. Barbiellini, M.G. Baring, D. Bastieri, R. Bellazzini, B. Berenji, E. Bissaldi et al. (Fermi-LAT Collaboration), *The Astrophysical Journal* **861**, 85 (2018)
- [11] J. Aasi, B.P. Abbott, R. Abbott, T. Abbott, M.R. Abernathy, K. Ackley, C. Adams, T. Adams, P. Addesso, R.X. Adhikari et al. (LIGO Collaboration), *Classical and Quantum Gravity* **32**, 074001 (2015)
- [12] F. Acernese, M. Agathos, K. Agatsuma, D. Aisa, N. Allemandou, A. Allocca, J. Amarni, P. Astone, G. Balestri, G. Ballardin et al. (Virgo Collaboration), *Classical and Quantum Gravity* **32**, 024001 (2015)
- [13] H. Abe, T. Akutsu, M. Ando, A. Araya, N. Aritomi, H. Asada, Y. Aso, S. Bae, R. Bajpai, K. Cannon et al. (KAGRA Collaboration), *Galaxies* **10**, 63 (2022)
- [14] M. Ahlers, K. Helbing, C.P. de los Heros, *The European Physical Journal C* **78**, 924 (2018)
- [15] S. Adrián-Martínez, M. Ageron, F. Aharonian, S. Aiello, A. Albert, F. Ameli, E. Anasontzis, M. Andre, G. Androulakis, M. Anghinolfi et al. (KM3NeT Collaboration), *Journal of Physics G: Nuclear and Particle Physics* **43**, 084001 (2016)
- [16] L. Fariña, L. Jouvin, J. Rico, N. Mori, F. Gargano, V. Formato, F. de Palma, C. Pizzolotto, J. Casaus, M.N. Mazziota et al., *PoS ICRC2021*, 651 (2021)
- [17] L. Pacini, O. Adriani, Y. Bai, T. Bao, E. Berti, S. Bottai, W. Cao, J. Casaus, X. Cui, R. D’Alessandro et al., *PoS ICRC2021*, 066 (2021)
- [18] O. Adriani, M. Antonelli, A. Basti, E. Berti, P. Betti, G. Bigongiari, L. Bonechi, M. Bongi, V. Bonvicini, S. Bottai et al., *Journal of Instrumentation* **17**, P09002 (2022)
- [19] C. Perrina, P. Azzarello, F. Cadoux, Y. Favre, J.M. Frieden, D. La Marra, D. Sukhonos, X. Wu, *PoS ICRC2021*, 067 (2021)
- [20] A. Sanmukh, S. Gómez, A. Comerma, J. Mauricio, R. Manera, A. Iraola, A. Sanuy, X. Wu, P. Azzarello, C. Perrina et al., in *2021 IEEE Nuclear Science Symposium and Medical Imaging Conference (NSS/MIC)* (2021), pp. 1–3
- [21] D. Kyratzis, F. Alemanno, C. Altomare, P. Bernardini, P. Cattaneo, I. De Mitri, F. de Palma, L. Di Venere, M. Di Santo, P. Fusco et al., *PoS ICRC2021*, 054 (2021)
- [22] B. Huang, H. Liu, X. Huang, M. Xu, Y. Dong, X. Wei, X. Liu, H. Feng, Q. Yang, J. Gu et al., *Nuclear Instruments and Methods in Physics Research Section A: Accelerators, Spectrometers, Detectors and Associated Equipment* **962**, 163723 (2020)